

Computational Analysis of the Effect of Cardiac Motion on Left Main Coronary Artery Hemodynamics

Laila Fadhillah Ulta Delestri¹, Foo Ngai Kok², Amr Al Abed³, Socrates Dokos⁴, Mohd Jamil Mohamed Mokhtarudin⁵, Neil W Bressloff⁶, Azam Ahmad Bakir⁷

^{1,2,7}University of Southampton Malaysia, Johor, Malaysia

^{3,4}University of New South Wales, Sydney, Australia

⁵Universiti Malaysia Pahang, Pahang, Malaysia

⁶University of Southampton, Southampton, United Kingdom

Abstract

Cardiac muscle health is dependent on the adequate supply of oxygenated blood and nutrients to ensure optimal cardiac function, avoiding ischemia. The continuous supply of oxygenated blood occurs mainly through coronary arteries embedded within the muscle. Cardiac ventricular motions involve twisting, contracting and expanding, giving rise to the biomechanical behavior of the coronary arteries. The goal of this work is to study the impact of cardiac motion on the coronary flow dynamics using a two-way fluid-structure interaction. Blood flow was modelled within an idealized 3D coronary arterial structure using incompressible laminar Navier-Stokes equations. This study was conducted on a left main artery in which the vessel walls were represented using an isotropic five-parameter Mooney-Rivlin hyperelastic material deformed dynamically with prescribed displacement boundary conditions to simulate the torsional and expansion motions. Results have shown that the bifurcation region in moving artery produced higher velocities than in the non-moving case, particularly during systolic torsional motion. During systole, the wall shear stress near the bifurcation was found to be lower in the non-moving case relative to the moving one. In the non-moving model, a helical-shaped pattern of secondary flow was observed as the blood flowed through the curved vessel. However, this pattern diminished in the moving model, where the arterial curvature dynamically changed throughout the cardiac cycle. Overall, it is necessary to include cardiac motion when modelling coronary vessels' hemodynamics.

1. Introduction

Coronary artery disease (CAD) is the most common cardiac disease and the leading cause of death globally. An estimated nearly 18 million people died from CAD in

2019 [1]. Since coronary arteries are attached to the cardiac epicardial surface, any abnormal motion of cardiac muscle can potentially affect the vascular hemodynamics including blood emptying and filling. Studies on the mechanical interaction between the myocardium and coronary arteries are well-documented [2-4]. Large torsional motion, wall thickening and contraction dynamics of the ventricles are expected to alter the hemodynamic environment within the coronary arteries.

Arterial motion has been shown to function as a pump that drives blood into the artery [4]. These works studied the effect of myocardial motion on coronary blood flow [5,6] and revealed that the impact of cardiac motion on time-averaged wall shear stress (WSS) was insignificant compared to oscillatory hemodynamic parameters such as temporal variation of WSS and oscillatory shear index. Gholipour et al. [7] observed a significant effect of cardiac motion on the von-Mises stress of the coronary artery which leads to a 265% increase in radial stress. Other studies [8,9] concluded that the effect of dynamic vessel motion was only secondary to the pulsatile flow effects on the coronary arteries.

Most of these studies have only considered a small section of a coronary artery with no branching and have not investigated in depth the combination of ventricular torsion and expansion on the coronary hemodynamics. In reality, cardiac motion is likely to be spatially inhomogeneous and therefore the embedded arteries are subject to deformations in the radial, circumferential and longitudinal directions [10]. Moreover, the role of secondary flow patterns in moving coronary vessels has not yet been investigated. The present study simulated a physiologically deforming motion in an idealized arterial geometry and compared the hemodynamic effects against the non-moving case.

2. Methods

An idealized model of left main coronary artery bifurcated 45° into the left anterior descending and left circumflex arteries has been adopted [11], as in Figure 1.

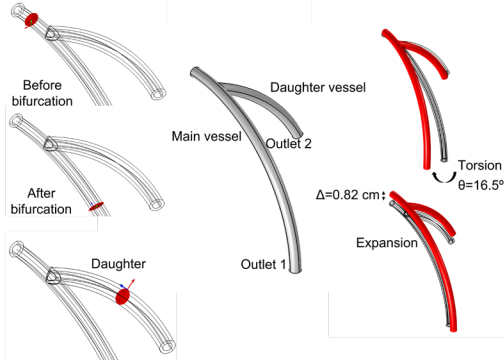


Figure 1. Idealized geometry of left main artery, selected cross-sections for analysis and the prescribed motions.

The temporal variations of coronary arterial deformations are referred to as the combination of sideway twists and outward radial displacements corresponding to ventricular systolic twisting motion and diastolic expanding motion. Boundary conditions for the solid mechanic's deformations were set so that both the inlet and outlet boundaries are sliding in-plane. The rotation angle was a maximum of 16.5° [12] to the coronary outlet of the main vessel (Outlet 1) while the maximum arterial wall displacement during expansion was 0.82 cm [13]. Figure 2 shows the pulsatile inlet velocity [14] and the prescribed motion activation functions [15] imposed on the artery model. Our present study implemented the effects of torsion (TORSION) and expansion (EXPANSION) separately, as well as their combination (COMBINED) in a complete cardiac cycle. Figure 3 depicts the effect of combined torsional and translational motion at different time points in the cardiac cycle.

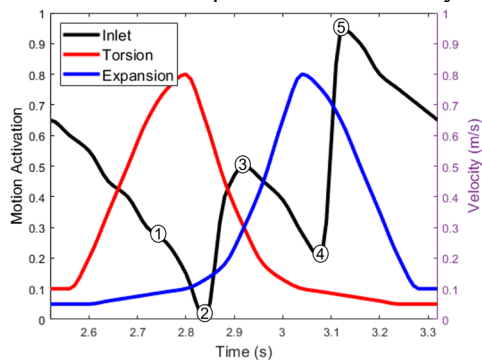


Figure 2. Inlet pulsatile coronary velocity and the motion activation functions along a cardiac cycle. (1) End of diastole (T=2.76s), (2) Reversed flow in early systole (T=2.84s), (3) Local maximum systole (T=2.91s), (4) Local minimum systole (T=3.07s) and (5) Maximum flow at beginning of diastole (T=3.13s).

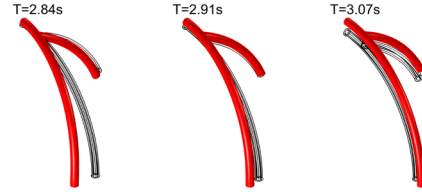


Figure 3. The effect of combined torsional and translational motion on the position of the coronary artery at different time points.

The arterial walls were assumed to be homogeneous, incompressible and isotropic. We employed a five-parameter Mooney-Rivlin hyperelastic constitutive equation [11]. Blood flow through the coronary artery was treated as Newtonian, laminar and incompressible. The standard Navier-Stokes formulations we used are given in Eqs. (1) and (2).

$$\rho \frac{\partial \mathbf{v}}{\partial t} + \rho (\mathbf{v} \cdot \nabla) \mathbf{v} = -\nabla \cdot (-p\mathbf{I} + \mu(\nabla \mathbf{v} + (\nabla \mathbf{v})^T)) \quad (1)$$

$$\nabla \cdot \mathbf{v} = 0 \quad (2)$$

where p is the fluid pressure, \mathbf{v} is fluid velocity, ρ is blood density set to 1050 kg/m³ and μ is dynamic viscosity set to 0.00345 Pa.s [14]. A zero-pressure boundary condition was defined at both outlets and a no-slip boundary condition was applied to the inner wall of the arteries.

The models were meshed using quadratic tetrahedral elements in COMSOL Multiphysics v5.6 (COMSOL AB, Sweden). Uniform meshes were considered for both solid and fluid domains with local grid refinement applied at the bifurcation region as intense variations of the flow field were expected in this area. To improve the simulation accuracy while maintaining an optimum computational time, a mesh convergence study was conducted using three different mesh configurations, normal mesh (106794 elements), fine mesh (215921 elements) and extra fine mesh (1658458 elements). The WSS across a cardiac cycle has been used as the convergence criteria and resulted in the fine mesh having less than a 6% error difference hence it is sufficient for the simulation with a satisfactory outcome. The simulation used a Parallel Direct Sparse Solver with a second-order Backward Differentiation Formula time-stepping scheme with an output time step of 10 ms. To acquire a stable and consistent result, all simulations were run for four cardiac cycles with a period set to 800 ms equivalent to a resting heart rate of 75 beats per minute. Data for the analysis was obtained from the last cardiac cycle.

3. Results and discussion

The blood flow velocity magnitude, shown in Figure 4 is slightly greater in the (EXPAND) and (COMBINED) cases, while the non-moving and (TORSION) cases

produce a very similar blood velocity profile. This is attributed to the fact that the displacement imposed in (EXPAND) case is larger than that of the (TORSION) case, whereby the overall displacement caused by the twisting effect is insignificant.

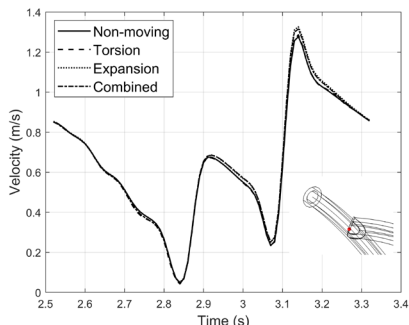


Figure 4. Comparison of blood velocity profile throughout a cardiac cycle taken at a point on the bifurcation of the main artery.

Physiologically, maximum coronary flow rate occurs during diastole, whilst the flow rate is lowest during systole since the coronary artery is compressed and twisted by the contracting myocardium [2]. According to Figure 5 (Top), during maximum systole, all cases demonstrated a sharp drop in WSS at the bifurcation and then followed by a gradual increase after the bifurcation region towards the outlet of the main artery. Among all cases considered, the (TORSION) was found to be the strongest effect at the bifurcation region due to the twisting motion and it activated maximally at this time point. During the minimum systole in Figure 5 (Bottom), the WSS is observed in similar patterns where all cases had the lowest WSS at the bifurcation zone. However, the effect of wall displacement on the local WSS appears to be much stronger compared to the maximum systolic phase. WSS near the inlet of (EXPANSION) and (COMBINED) cases are found to be greater than in the non-moving case. The WSS at the bifurcation region of the (COMBINED) case is noticeable at about 1.5-fold lower than in the non-moving case but ended with a WSS larger than the non-moving case at the end of the artery. The change in the WSS slopes is a consequence of the dominant inertial effect caused by the displacement of the vascular wall that results in a change of the local flow field.

We also investigate the characteristics of the secondary flow in the motion-induced coronary artery in Figure 6. Due to high fluid velocity, coronary artery experiences a centrifugal force that formed a pair of counter-rotating vortices known as Dean vortices [16]. Before the bifurcation, the non-moving case set off symmetric Dean vortices. Further downstream, after the bifurcation, the vortices are disturbed and a swirling effect can be seen. The vortices patterns also appear in the daughter's vessel but in the opposite (horizontal) direction. However, in the (COMBINED) case, the vortices appear to have been

eliminated and become non-symmetric in all cross-sections of the vessel regardless of cardiac cycle phases. The symmetric vortices are washed out by the motion of the artery causing the blood to move sideways and in the outward radial direction.

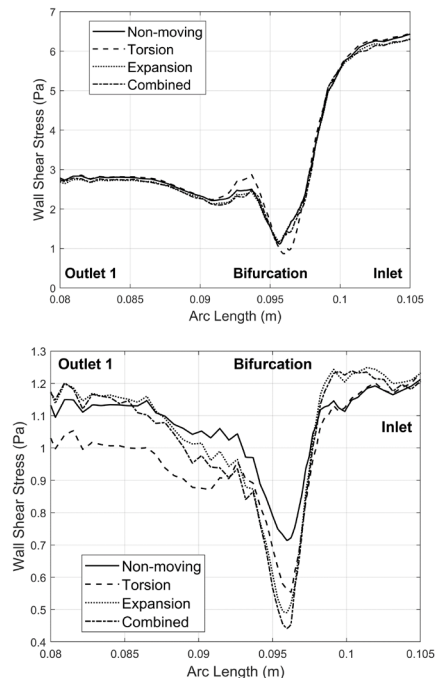


Figure 5. Variation of WSS profiles along the bifurcation region of the main vessel. (Top) Maximum systole ($T=2.91s$) and (Bottom) Minimum systole ($T=3.07s$).

The results suggested that the reduced and the absence of symmetric Dean vortices in moving cases are associated with additional energy supplied onto the flow field of the coronary artery through the twisting and expanding motions. These motions fostered the blood flow field to skew throughout the artery, suppressing the low WSS region which leads to changes in the local flow field and the corresponding blood shear stress. These findings comprehend that arterial motion has an appreciable effect on the movement of blood inside the artery and may influence the hemodynamics of the artery.

Several limitations of the study must be noted. For simplicity, we employed an idealized coronary artery geometry with a single branch. Further, our zero-pressure outlet condition may not be representative of the real afterload condition of a coronary artery. Nevertheless, this work is relevant as a preliminary basis to understand the influence of complex cardiac motion on coronary arterial blood flow.

4. Conclusion

This study explored the effect of deforming idealized arterial geometry, mimicking the twisting and expanding

motion of cardiac ventricles on the coronary artery flow. With the assistance of arterial motions, the deforming structure undergoes significant displacement. These motions altered the WSS magnitude particularly at the bifurcation relative to non-moving artery. Also, the moving artery was shown to abolish the rotating helical pattern in the secondary flow.

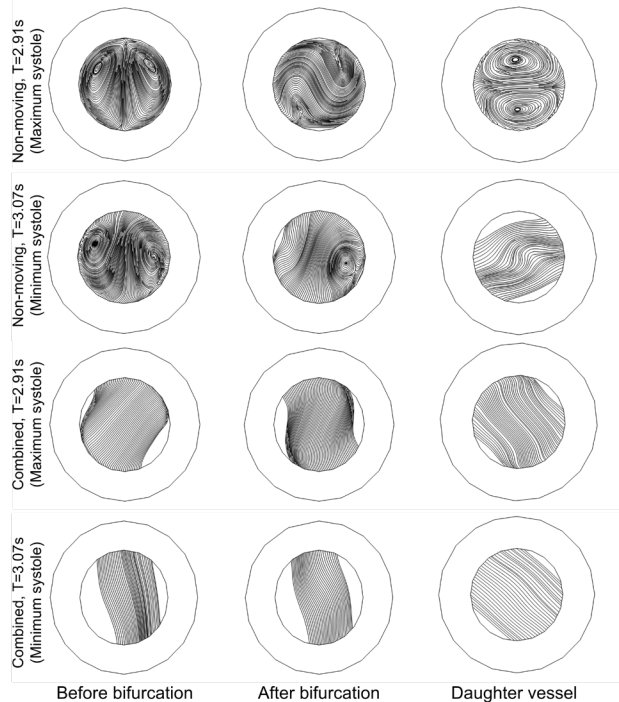


Figure 6. Velocity streamlines of secondary flow in non-moving and combined case in three chosen cross-section planes.

Acknowledgments

This project is supported by the Malaysian Ministry of Higher Education Fundamental Research Grant Scheme (FRGS)-FRGS/1/2020/TK0/USMC/02/5. LFUD is also sponsored by University of Southampton Studentship.

References

- [1] Cardiovascular diseases: World Health Organization (WHO); 2021 [Available from: https://www.who.int/health-topics/cardiovascular-diseases#tab=tab_1].
- [2] Westerhof N, Boer C, Lamberts RR, Sipkema P. Cross-Talk Between Cardiac Muscle and Coronary Vasculature. *Physiological Reviews*. 2006;86(4):1263-308.
- [3] Fan L, Namani R, Choy JS, Kassab GS, Lee LC. Effects of Mechanical Dyssynchrony on Coronary Flow: Insights From a Computational Model of Coupled Coronary Perfusion With Systemic Circulation. *Frontiers in Physiology*. 2020;11.
- [4] Lee J, Smith NP. The multi-scale modelling of coronary blood flow. *Annals of biomedical engineering*. 2012;40(11):2399-413.
- [5] Forouzandeh F, Fatourae N, editors. Effects of Cardiac Motion on the Flow Rate of the Left Coronary Artery Considering Different Blood Viscosities. 2017 24th National and 2nd International Iranian Conference on Biomedical Engineering (ICBME); 2017 30 Nov.-1 Dec. 2017.
- [6] Biglarian M, Firoozabadi B, Saidi MS. Atheroprone sites of coronary artery bifurcation: Effect of heart motion on hemodynamics-dependent monocytes deposition. *Comput Biol Med*. 2021;133:104411.
- [7] Gholipour A, Ghayesh MH, Zander A, Mahajan R. Three-dimensional biomechanics of coronary arteries. *International Journal of Engineering Science*. 2018;130:93-114.
- [8] Kolandavel MK, Freund E-T, Ringgaard S, Walker PG. The effects of time varying curvature on species transport in coronary arteries. *Annals of biomedical engineering*. 2006;34(12):1820-32.
- [9] Wang J, Paritala PK, Mendieta JB, Komori Y, Raffel OC, Gu Y, et al. Optical coherence tomography-based patient-specific coronary artery reconstruction and fluid-structure interaction simulation. *Biomech Model Mechanobiol*. 2020;19(1):7-20.
- [10] Aghajankhah MR, Hosseinpour M, Moladoust H, Rad MA, Nasiri E. Evaluation of Left Ventricular Longitudinal, Radial, and Circumferential Strains in Subjects with Normal Variations of Coronary Dominance: A Preliminary Comparative Study. *Anatol J Cardiol*. 2022;26(8):645-53.
- [11] Jahromi R, Pakravan HA, Saidi MS, Firoozabadi B. Primary stenosis progression versus secondary stenosis formation in the left coronary bifurcation: A mechanical point of view. *Biocybernetics and Biomedical Engineering*. 2019;39(1):188-98.
- [12] Stöhr EJ, Shave RE, Baggish AL, Weiner RB. Left ventricular twist mechanics in the context of normal physiology and cardiovascular disease: a review of studies using speckle tracking echocardiography. *Am J Physiol Heart Circ Physiol*. 2016;311(3):H633-44.
- [13] Shechter G, Resar JR, McVeigh ER. Displacement and velocity of the coronary arteries: cardiac and respiratory motion. *IEEE Trans Med Imaging*. 2006;25(3):369-75.
- [14] Chen X, Zhuang J, Huang H, Wu Y. Fluid-structure interactions (FSI) based study of low-density lipoproteins (LDL) uptake in the left coronary artery. *Scientific Reports*. 2021;11(1):4803.
- [15] Andersson DC, Betzenhauser MJ, Marks AR. Chapter 12 - Excitation-Contraction Coupling in the Heart. In: Hill JA, Olson EN, editors. *Muscle*. Boston/Waltham: Academic Press; 2012. p. 153-9.
- [16] Kalpakli A, Örlü R, Alfredsson PH. Dean vortices in turbulent flows: rocking or rolling? *Journal of Visualization*. 2012;15(1):37-8.

Address for correspondence:

Azam Ahmad Bakir.
University of Southampton Malaysia, C0301, C0302, C0401,
Blok C Eko Galleria, 3, Jalan Eko Botani 3/2, Taman Eko
Botani, 79100 Nusajaya, Johor, Malaysia.
A.Ahmad-Bakir@soton.ac.uk